Clinical Radiology 74 (2019) 651.e15–651.e23

Contents lists available at ScienceDirect

Clinical Radiology

journal homepage: www.clinicalradiologyonline.net

Grading meningiomas using mono-exponential, bi-exponential and stretched exponential model-based diffusion-weighted MR imaging

L. Lin [a], Y. Xue [b], Q. Duan [b], X. Chen [c], H. Chen [d], R. Jiang [b], T. Zhong [b], G. Xu [e], D. Geng [a,**], J. Zhang [a,*]

[a] *Department of Radiology, Huashan Hospital, Fudan University, No.12 Wulumuqi Road (Middle), Jingan District, Shanghai, China*
[b] *Department of Radiology, Fujian Medical University Union Hospital, 29 Xinquan Road, Gulou District, Fuzhou, Fujian, China*
[c] *Department of Radiology, Fujian Cancer Hospital & Fujian Medical University Cancer Hospital, 240 Fuma Road, Jinan District, Fuzhou, Fujian, China*
[d] *Department of Pathology, Fujian Medical University Union Hospital, 29 Xinquan Road, Gulou District, Fuzhou, Fujian, China*
[e] *Department of Management Science, University of Miami, Coral Gables, FL, USA*

ARTICLE INFORMATION

Article history:
Received 5 July 2018
Accepted 3 April 2019

AIM: To prospectively evaluate and compare the potential of various diffusion metrics obtained from mono-exponential model (MEM), bi-exponential model (BEM), and stretched exponential model (SEM)-based diffusion-weighted imaging (DWI) in the grading of meningiomas.

MATERIAL AND METHODS: Consecutive 93 patients with histopathologically confirmed meningiomas received DWI of multiple b-values. Apparent diffusion coefficient (ADC), pure molecular diffusion (D), pseudo-diffusion coefficient (D*), perfusion fraction (*f*), water molecular diffusion heterogeneity index (alpha), and distributed diffusion coefficient (DDC) were calculated and compared between low-grade and high-grade meningiomas. Receiver operating characteristic and multivariable stepwise logistic regression analyses were performed to evaluate the diagnostic performance of different parameters.

RESULTS: The mean and normalised ADC, D, *f*, and DDC values were significantly lower in high-grade meningiomas than those in low-grade meningiomas (all $p<0.05$). The AUCs of D and DDC were significantly higher than that of *f* in the differentiation (all $p<0.05$). D was the only variable that could be used to independently differentiate high-grade and low-grade meningiomas ($p<0.001$).

CONCLUSION: Different models of DWI, including MEM, BEM, and SEM, are useful in the differentiating high-grade and low-grade meningiomas; however, D obtained from BEM is the most promising diffusion parameter for predicting the grade of meningiomas.

* Guarantor and correspondent: J. Zhang, Department of Radiology, Huashan Hospital, Fudan University, No.12 Wulumuqi Road (Middle), Jingan District, Shanghai, China. Tel.: +8621 5288 8338; fax: +8621 6248 9191.
** Guarantor and correspondent: D. Geng, Department of Radiology, Huashan Hospital, Fudan University, No.12 Wulumuqi Road (Middle), Jingan District, Shanghai, China. Tel.: +8621 5288 8338; fax: +8621 6248 9191.
E-mail addresses: gengdy@163.com (D. Geng), zhj81828@163.com (J. Zhang).

https://doi.org/10.1016/j.crad.2019.04.007
0009-9260/

Introduction

Meningiomas are one of the most common primary brain tumours and are classified into three grades according to the World Health Organization (WHO).[1] Most meningiomas correspond to low-grade lesions (Grade I), and the remaining are high-grade tumours (Grade II/III).[1,2] Low-grade tumours usually grow slowly and have favourable outcomes, whereas high-grade lesions are clinically and histologically aggressive with lower overall survival rates.[3,4] In addition, low-grade meningiomas located in high-risk intracranial areas, such as skull base, may be more suitable for long-term follow-up or stereotactic radiotherapy rather than surgery.[5] Thus, accurate grading is crucial to determine therapeutic strategies and to evaluate the prognosis.[6] Although conventional magnetic resonance imaging (MRI) provides several identifiable features for meningiomas, no specific feature has been found to be reliable in predicting the grade of the tumor.[7,8]

Apparent diffusion coefficient (ADC) obtained from diffusion-weighted imaging (DWI) with a mono-exponential model (MEM) has been widely used to grade meningiomas[9–12]; however, the values of ADC in grading meningiomas remain controversial. One possible explanation is that MEM does not consider the influence of the microcirculation of blood in capillaries, which may lead to inaccurate measurement of the diffusion.[13] Additionally, MEM assumes that water diffusion follows a Gaussian distribution; however, the complexity of biological tissue leads to restricted diffusion of water molecules, which leads to a non-Gaussian distribution.

Recently, several recent studies suggested that bi-exponential and stretched exponential DWI models might provide more accurate information about water diffusion.[14–16] The bi-exponential model (BEM) might allow separation of simple diffusion and microvascular perfusion, and it can provide three parameters: pure molecular diffusion (D), pseudo-diffusion coefficient (D*), and perfusion fraction (*f*).[17,18] D represents the perfusion-free diffusion in the coherent motion, D* describes macroscopically the incoherent movement of blood in the microvasculature compartment, and *f* denotes the fraction of the incoherent signal that arises from the vascular compartment in each voxel over the total incoherent signal.[19] Several studies have demonstrated that the diffusion parameters derived from BEM might be superior to ADC in predicting the grade of a tumour, including sinonasal, renal, and breast lesions[20–22]; however, relevant studies on meningiomas are limited.[10] The stretched exponential model (SEM) can give information on the diffusion and tissue heterogeneity by measuring the signal deviation from the mono-exponential behaviour caused by pseudo-perfusion effects.[23] Based on SEM, the parameters of distributed diffusion coefficient (DDC) and water diffusion heterogeneity index (alpha) can be achieved. The DDC represents the mean intravoxel diffusion rate and thus provides a more accurate measure of tissue diffusion. Alpha measures the average difference between apparent water diffusion rates and thus reflects microstructural heterogeneity. SEM has been widely used in various tumours such as gliomas, nasopharyngeal carcinomas (NPC), prostate, and ovarian tumours.[14,16,24,25] Although it was shown to be potentially valuable in grading gliomas, the application of SEM in meningiomas is still lacking.

In general, BEM and SEM are both non-Gaussian diffusion models and can accurately characterise tumour cellularity; however, BEM provides additional information on tissue microcirculation while SEM evaluates extra tumour properties of heterogeneity. As different models of DWI may provide information regarding different aspects of tissue properties, it may be valuable to explore their roles in the grading of meningiomas; however, to date, no comparison of these three different models of DWI in the identification of meningioma grade has been explored. The purpose of this study was to evaluate and compare the potential of various diffusion metrics obtained from MEM, BEM, and SEM DWI in the grading of meningiomas.

Materials and methods

Patients

This prospective study was approved by the local ethics and institutional review board committee and informed consent was obtained from every patient before participation. Patients with suspected meningiomas based on imaging support prior to referral to neurosurgery were recruited consecutively in a tertiary hospital from October 2014 to July 2017 (Fig 1). The inclusion criteria were as follows: (a) patients had multiple-b-value DWI; (b) tumours were histopathologically confirmed as meningiomas based on the 2016 WHO classification of tumours of the central nervous system[1]; (c) surgical resection was performed within 10 days after the MRI examination. The exclusion criteria were the following: (a) patients with any previous relevant treatment; (b) MRI data presented motion artefacts

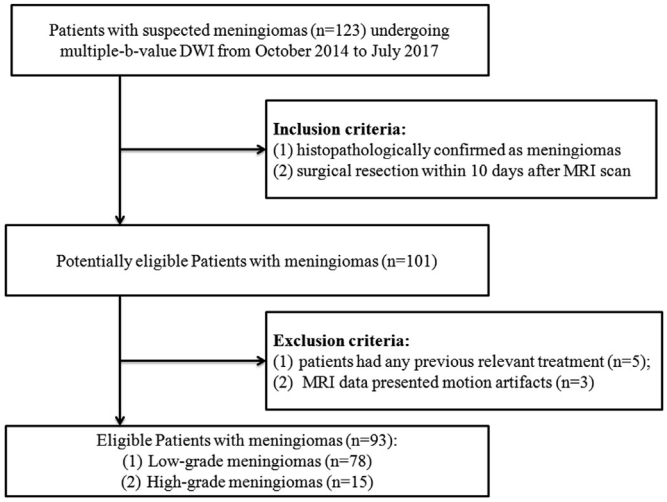

Figure 1 Patient flowchart.

(obvious images blurring or conspicuous movements among the sections of different b-values in the same acquisition location). A total of 123 patients received conventional MRI and multiple-b-value DWI, 110 patients underwent surgery in Union Hospital, and 101 patients with meningiomas were diagnosed via histopathology. Five patients were excluded due to previous relevant treatment (including radiotherapy, chemotherapy, or surgery), and three patients were excluded because of excessive head movement artefacts that significantly degraded image quality. Finally, 93 patients were included.

Image acquisition

MRI was performed using a 3 T MRI system (Discovery 750, GE Healthcare, Milwaukee, Wis, USA) equipped with a gradient system capable of a maximal amplitude of 50 mT/m and an eight-channel receiver head coil. Conventional non-enhanced MRI sequences, multiple-b-value DWI, and contrast-enhanced T1-weighted imaging were performed in sequence. The total scan duration was 15 minutes 41 seconds.

Conventional non-enhanced MRI sequences included axial T1-weighted fluid attenuated inversion recovery (FLAIR) images (repetition time [TR]=1,750 ms, echo time [TE]=23 ms, section thickness=5 mm, intersection gap=1.5 mm, field of view [FOV]=24 cm, matrix=320×320); axial T2-weighted FSE images (TR=6,488, TE=94 ms, section thickness=5 mm, intersection gap=1.5 mm, matrix=512×512, FOV=24 cm); axial T2-weighted FLAIR images (TR=8,500, TE=143 ms, section thickness=5 mm, intersection gap 1.5 mm, matrix=288×224, FOV=24 cm).

DWI used a spin echo (SE)-echo planar imaging (EPI) diffusion sequence in the axial plane (TR=5,000, TE=84.6 ms, section thickness=5 mm, intersection gap=0 mm, FOV=24 cm, matrix=192×192, number of sections=30. Twelve b-values from 0 to 3,000 s/mm^2 (0, 50, 100, 150, 200, 300, 500, 800, 1,000, 1,500, 2,000, and 3,000 s/mm^2; with number of excitations [NEX]=1 for b=0–500 s/mm^2, two NEX for b=800–1,000 s/mm^2, three NEX for b=1,500 s/mm^2, four NEX for b=2000 s/mm^2, and six NEX for b=3000 s/mm^2; varying diffusion gradient strength with constant pulse length [32 ms] and separation [49 ms]) were used in three orthogonal directions.

A contrast-enhanced three-dimensional (3D) axial T1-weighted fast spoiled gradient echo (FSPGR) was served as anatomical reference for DWI (TR=8.2, TE=3.2 ms, section thickness=1 mm, matrix=256×256, FOV=24 cm, inversion time [TI]=450 ms, flip angle=12°). Post-contrast images were performed after administration of intravenous contrast material (0.1 mmol/kg, gadopentetate dimeglumine, Bayer Schering, Berlin, Germany) at a speed of 2 ml/s.

Image processing

The DWI data were obtained and transferred to a workstation (Advantage Workstation 4.6; GE Medical Systems) for processing. Parameter maps were generated by the MADC program in the Functool software for each model.

The mono-exponential model was calculated using the equation

$$S(b)/S_0 = \exp(-b \times ADC)$$

where S(b) is the mean signal intensity with diffusion gradient b, and S_0 is the mean signal intensity without diffusion gradient.[26] In this study, two ADC metrics ($ADC_{0,1000}$ and ADC_{all}) were derived from the mono-exponential model. The difference between the $ADC_{0,1000}$ and ADC_{all} is that $ADC_{0,1000}$ is calculated by only two b-values (0,1000 s/mm^2) while the ADC_{all} is calculated by all 12 b-values.

The BEM was calculated using the equation

$$S(b)/S_0 = [f \times \exp(-b \times D^*)] + [(1-f) \times \exp(-b \times D)]$$

where D is the pure molecular diffusion. D* is the pseudo diffusion coefficient, *f* is the microvascular volume fraction representing the fraction of diffusion linked to microcirculation.[13]

The SEM was calculated using the equation

$$S(b)/S_0 = \exp[-(b \times DDC)^{alpha}]$$

where DDC is the distributed diffusion coefficient reflecting the mean intravoxel diffusion rate, and alpha corresponds to intravoxel water diffusion heterogeneity ranging between 0 and 1.[23]

For MEM, data were fitted using the least square fit for linear fitting and for the BEM and SEM, data were fitted using the Levenberg–Marquardt fit for nonlinear fitting.[14,21] The quantitative measurement of parameter maps was performed on ImageJ (version 1.50i; US NIH). A semi-automatic ROI setting method was performed, in line with former studies.[9,27] On contrast-enhanced T1-weighted imaging, an ROI was drawn to include the entire enhancing lesion on the largest section of a tumour. Regions of visual cyst, necrosis, haemorrhage, and calcifications were carefully avoided with reference to conventional MRI. Each ROI was semi-automatically delineated by using the wand tool in ImageJ and copied to parameter maps for analyses. A visual check of the positioning of the ROI on the parametric maps was further performed. Similarly, an ROI of normal appearing white matter (NAWM) was created in the contralateral centrum semiovale in accordance with former studies.[9,28] If a tumour was located on the midline, the ROI was set in the centrum semiovale of both hemispheres, and the mean value was used. Afterwards, mean diffusion values ($ADC_{0,1000}$, ADC_{all}, D, D*, *f*, DDC, alpha) in the tumours were normalised to the corresponding values in the contralateral NAWM to reduce inter-subject variation. Besides, the tumour size was also measured and defined as the maximum area on contrast-enhanced T1-weighted imaging. Each image was analysed independently by two blinded neuroradiologists (with 6 and 10 years' experience), and the average values of two readers were used for analysis.

In addition, the mean signal-to-noise ratios (SNRs) in the lesions and NAWM for b=3,000 s/mm^2 images were calculated to be 56.2–197.8 and 70.7–224, respectively.[29] Thus, the SNR was large enough to ensure proper depiction of the signal.

Statistical analysis

SPSS software (Version 19.0, IBM, Armonk, NY, USA) and MedCalc software (https://www.medcalc.org/, version 11.4.2.0) were used for statistical analyses. The inter-reader reliability for parameter measurements was assessed using an intra-class correlation coefficient (ICC) with 95% confidence intervals (CI). The Kolmogorov–Smirnov test was performed to analyse the normal distribution of all metrics. The demographic data and diffusion metrics were compared between high-grade and low-grade meningiomas with χ^2 test for categorical variables, independent-sample *t*-tests for normally distributed continuous variables, or Mann–Whitney *U*-tests for other continuous variables. Receiver operating characteristic curves were performed to determine the best diagnostic accuracy of mean and normalised diffusion parameters in the grading of meningiomas. The area under the curve (AUC), Youden index, sensitivity, specificity, positive predictive value (PPV), and negative predictive value (NPV) of each parameter were calculated. A multivariable stepwise logistic regression analysis of diffusion parameters was performed to determine the best predictors for grading meningiomas. *p*-Values <0.05 were considered significant for all the tests.

Results

A total of 93 patients, including 78 patients with low-grade meningiomas and 15 patients with high-grade meningiomas, were enrolled in this study. All patients received total resection, which was confirmed via postsurgical MRI. The subtypes of low-grade meningiomas included meningothelial meningiomas (n=23), fibrous meningiomas (n=22), transitional meningiomas (n=25), angiomatous meningiomas (n=6), secretory meningiomas (n=2), atypical meningiomas (n=13), and anaplastic meningiomas (n=2). Of these patients, 22 were males and 71 were females. The age of patients ranged from 19 to 79 years old, with a mean age of 54.4 years. The demographics of low-grade and high-grade meningiomas are summarised in Table 1.

As shown in Table 2, good inter-reader agreements were achieved in the measurement of diffusion parameters. Representative cases of low-grade and high-grade meningioma are shown in Figs 2 and 3, respectively. Table 3 and Fig 4 show the quantitative comparison of differences in diffusion parameters between the two meningioma groups. The mean and normalised ADC, D, *f*, and DDC values were significantly lower in high-grade meningiomas than those in low-grade meningiomas ($p<0.05$). There was no significant difference in the mean and normalised values of D* and alpha between the two groups ($p>0.05$).

The results of the receiver operating characteristic curves for mean and normalised diffusion parameters in grading meningiomas are summarised in Table 4 and Fig 5. D exhibited the maximal AUC for differentiating high-grade meningiomas from low-grade meningiomas. ADC_{all} and DDC had lower values, followed by $ADC_{0,1000}$ and *f*. As shown in Table 5, the AUCs of mean and normalised D, ADC_{all}, and DDC were significantly higher than those of $ADC_{0,1000}$ and *f* in differentiating between high-grade meningiomas and low-grade meningiomas ($p<0.05$). In addition, multivariable stepwise logistic regression analysis showed that the normalised D was the most significant variable, with a parameter estimate of 11.86 and a standard error of 3.01 ($p<0.001$).

Table 1
Clinical information and magnetic resonance imaging metrics for low-grade (LGM) and high-grade meningiomas (HGM).

	LGM	HGM	*p*-Value
n	78	15	
Age	53.49±9.8	58.87±14.28	0.107[a]
Sex (% male)	19 (24.36%)	3 (20%)	0.974[b]
Tumour size (mm^2)	1024.14±738.13	993.32±437.31	0.612[a]
Ki-67 LI	2.9±2.2	10.40±6.86	<0.001[a]

Data are presented as mean ± standard deviation or percentages, *n* (%).
Ki-67 LI: Ki-67 labelling index.
[a] Comparisons were performed by Mann–Whitney *U*-test.
[b] Comparisons were performed by χ^2 test.

Table 2
Inter-observer variability in measurements of meningiomas.

Region	Metrics	Intra-class correlation coefficient (95% CI for interobserver)
The solid region of the tumour	$ADC_{0,1000}$	0.978 (0.962–0.989)
	ADC_{all}	0.997 (0.995–0.998)
	D	0.995 (0.991–0.997)
	D*	0.970 (0.951–0.981)
	f	0.895 (0.832–0.934)
	DDC	0.995 (0.992–0.997)
	alpha	0.939 (0.903–0.962)
NAWM	$ADC_{0,1000}$	0.946 (0.914–0.960)
	ADC_{all}	0.970 (0.953–0.981)
	D	0.966 (0.946–0.979)
	D*	0.874 (0.799–0.921)
	f	0.916 (0.865–0.947)
	DDC	0.973 (0.958–0.983)
	alpha	0.940 (0.905–0.963)

CI, confidence interval; NAWM, normal-appearing white matter; ADC, apparent diffusion coefficient; D, pure molecular diffusion, D*, pseudo-diffusion coefficient; *f*, perfusion fraction; alpha, water molecular diffusion heterogeneity index; DDC, distributed diffusion coefficient, $ADC_{0,1000}$, ADC calculated using only two b-values (0,1000 s/mm^2); ADC_{all}, ADC calculated using all 12 b-values.

Discussion

DWI has received much attraction in the evaluation of intra-tumoural pathological patterns, including cellularity, microcirculation, and intra-tumoural heterogeneity.[30] MEM, BEM, and SEM are different exponential models based on multi-b values DWI. In this study, MEM, BEN, and SEM DWI were used to characterise the biological behaviour of meningiomas. The present

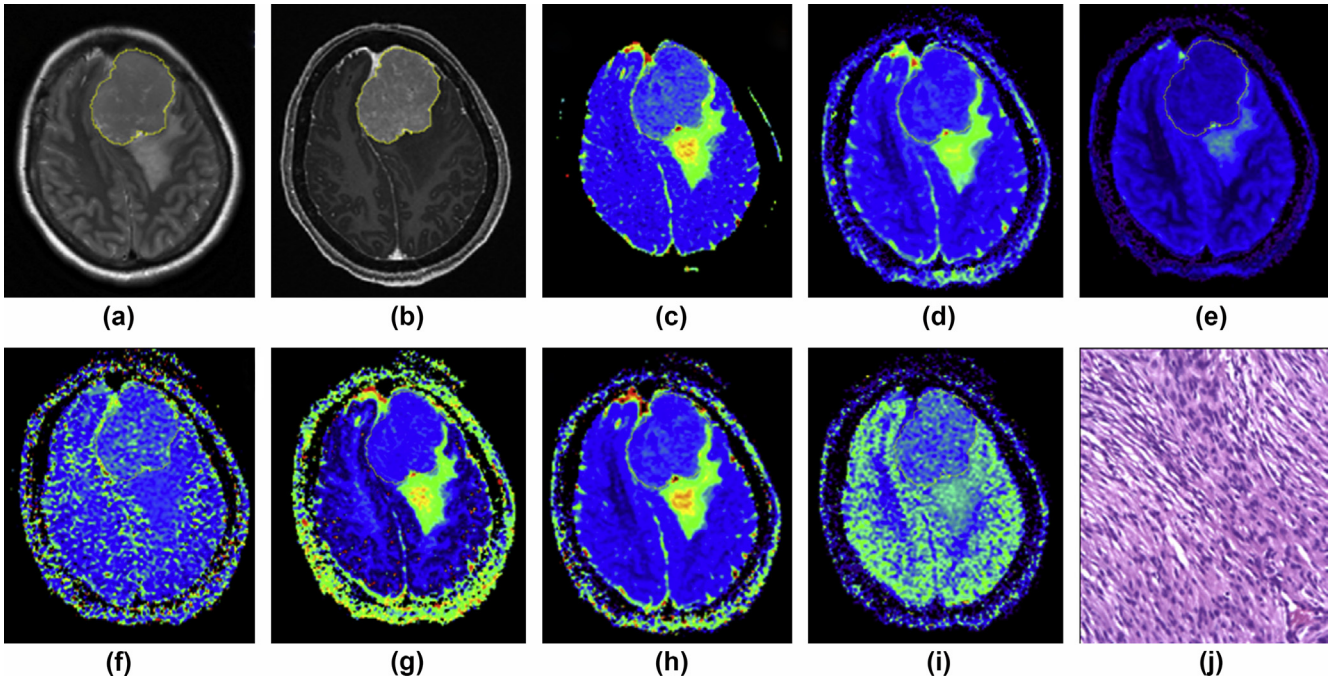

Figure 2 Low-grade meningioma in a 54-year-old woman. A mass was located in left cerebral convexity, demonstrating iso-intensity on T2-weighted imaging (a), and homogeneous enhancement on contrast-enhanced T1-weighted imaging (b). Compared with normal-appearing grey matter, the lesion shows isointensity on the $ADC_{0,1000}$ (c), ADC_{all} (d), D (e), D^* (f), *f* (g), DDC (h), and alpha (i) maps. Haematoxylin–eosin staining (j) confirmed the mass as a fibrous meningioma (magnification, ×100).

results demonstrated that the differentiation of low-grade and high-grade meningiomas is feasible by different models of DWI. Moreover, D and DDC generally performed better than *f*. In addition, D was the strongest independent predictor associated with the grade of meningiomas.

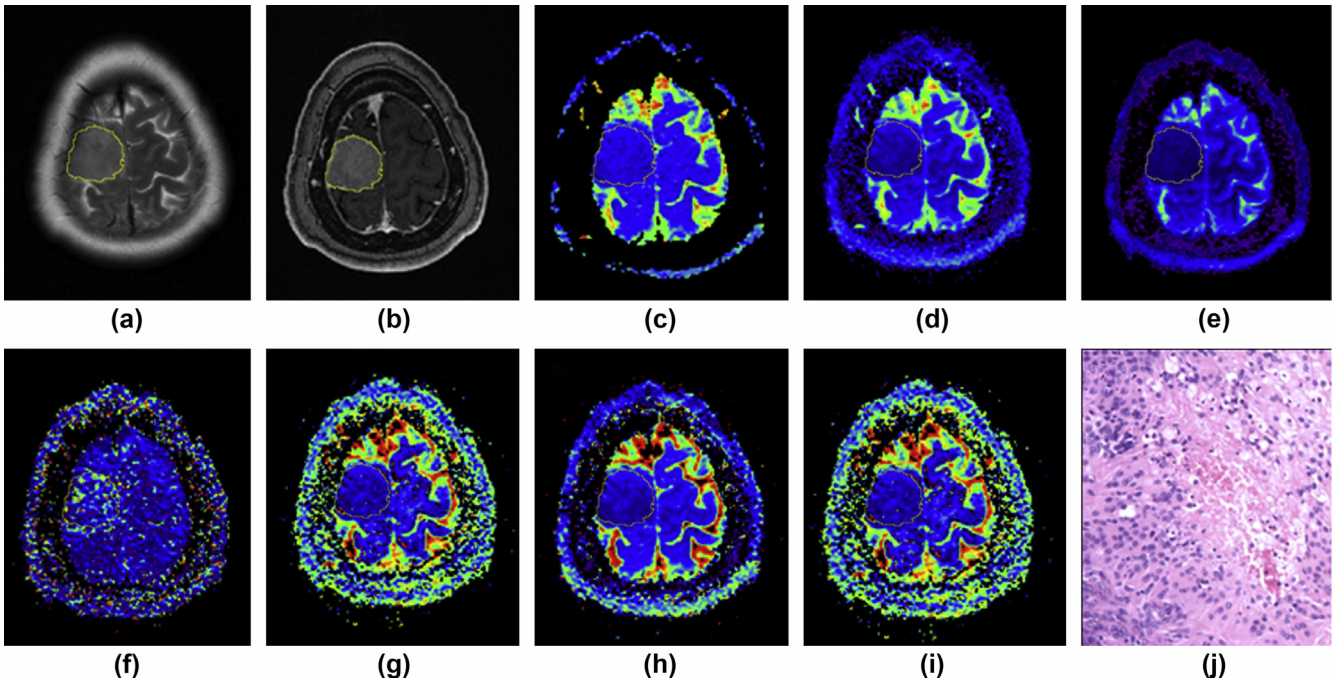

Figure 3 High-grade meningioma in a 44-year-old woman. A mass was located in the right cerebral convexity, demonstrating isointensity on T2-weighted imaging (a), and homogeneous enhancement on contrast-enhanced T1-weighted imaging (b). Compared with the normal-appearing grey matter, the lesion shows hypointensity on the $ADC_{0,1000}$ (c), ADC_{all} (d), D (e), *f* (g) and DDC (h) maps, slightly hyperintensity on the D^* (f) map and isointensity on the alpha (i) map. Haematoxylin–eosin staining (j) confirmed the mass as an atypical meningioma (magnification, ×100).

Table 3
Comparison of mean and normalised diffusion metric values between low-grade and high-grade meningiomas.

Values	$ADC_{0,1000}$	ADC_{all}	D	D*	*f*	DDC	alpha
Mean values							
Low-grade meningiomas	0.85±0.16	0.69±0.10	0.55±0.06	4.74±2.20	0.27±0.06	0.82±0.19	0.76±0.07
High-grade meningiomas	0.77±0.10	0.59±0.05	0.47±0.05	5.28±2.29	0.23±0.03	0.64±0.08	0.73±0.13
p-Value	<0.008[b]	<0.001[a]	<0.001[b]	0.329[b]	0.030[b]	<0.001[b]	0.336[a]
Normalised values							
Low-grade meningiomas	1.12±0.25	1.20±0.17	1.25±0.16	1.71±0.80	0.94±0.21	1.26±0.30	0.98±0.09
High-grade meningiomas	1.02±0.18	1.00±0.08	1.03±0.12	1.91±0.83	0.79±0.11	0.95±0.11	0.94±0.17
p-Value	<0.021[b]	<0.001[a]	<0.001[b]	0.347[b]	0.004[b]	<0.001[b]	0.360[a]

Data are presented as mean±standard deviation. $ADC_{0,1000}$, ADC_{all}, D, D*, and DDC are in units of $\times 10^{-3}$ mm^2/sec. See Table 2 for definitions of abbreviations.
[a] Comparisons were performed by independent samples *t*-test.
[b] Comparisons were performed by Mann–Whitney *U*-test.

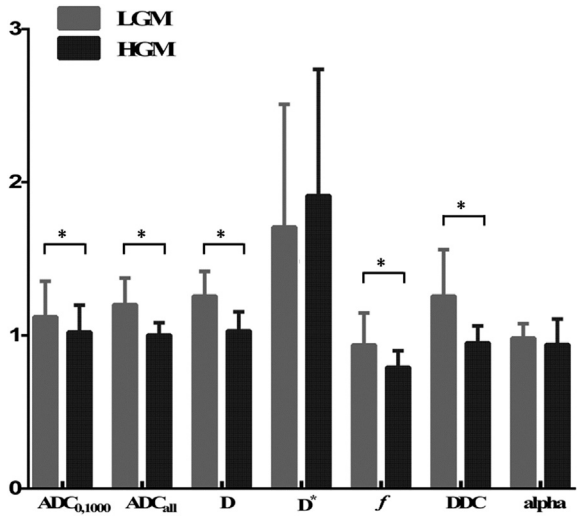

Figure 4 Comparisons of the normalised diffusion metrics between high-grade and low-grade meningiomas. Error bars=standard deviations across subjects. *$p<0.05$. LGM, low-grade meningiomas; HGM, high-grade meningiomas.

In the current study, ADC values derived from MEM were significantly lower in high-grade meningiomas. These are because ADC reflects the overall diffusion level and correlates with the cellular density of tumour tissue. Compared to the benign meningiomas, malignant tumour cells manifested as increased cellular density, reduced extracellular space, and higher nuclear/cytoplasmic ratio, which would lead to the decrease of ADC.[31] Recent research also revealed that the MEN can help to grade meningiomas.[9,11] According to Gihr *et al.*, ADC values of high-grading meningiomas were lower than those of low-grading meningiomas, which is consistent with the present results.[11] Similarly, Lin *et al.* found significantly lower ADC values in high-grade meningiomas than those in low-grade meningiomas.[9] In this study, a cut-off normalised ADC value of 1.047 has been identified in grading meningiomas, which is in good agreement with the value reported by Lin *et al.*[9]; however, some other studies also reported that ADC failed to evaluate the grade of meningiomas.[10,32] The contradictory findings between the current study and former research may be attributed to differences in enrolment bias and parameter settings. Moreover, in the current study, the ADC value calculated by fitting all 12 b-values had a higher diagnostic performance than that of the ADC value only calculated by two b-values. This is in concordance with the suggestion that MEM based on multiple b-values could avoid the selection bias of different b-values and achieve more reliable measurements.[33]

According to the present results, using the BEM DWI, the D values of high-grade meningiomas were remarkably lower than that of low-grade meningiomas, which was in line with a previous study.[10] BEM can separate the diffusion and perfusion component from overall diffusion

Table 4
Receiver operating characteristic curve results of diffusion metrics for differentiating low-grade from high-grade meningiomas.

Values	AUC	Cut-off value	Sensitivity	Specificity	Youden's index	PPV	NPV
Mean values							
ADC0,1000	0.718	0.787	65.38	80.00	45.38	94.4	30.8
ADCall	0.842	0.632	74.36	80.00	54.36	95.1	37.5
D	0.880	0.522	71.79	93.33	65.13	98.2	38.9
f	0.678	0.245	57.69	80.00	37.69	93.7	26.7
DDC	0.832	0.74	57.69	100.00	57.69	100.0	31.2
Normalised values							
ADC0,1000	0.689	0.986	78.21	66.67	44.87	92.4	37.0
ADCall	0.869	1.047	82.05	80.00	62.05	95.5	46.2
D	0.885	1.181	75.64	93.33	68.97	98.3	42.4
f	0.737	0.808	69.23	80.00	49.23	94.7	33.3
DDC	0.854	1.044	74.36	86.67	61.03	96.7	39.4

$ADC_{0,1000}$, ADC_{all}, D, and DDC are in units of $\times 10^{-3}$ mm^2/sec.
AUC, area under the curve; PPV, positive predictive value; NPV, negative predictive value. See Table 2 for definitions of abbreviations.

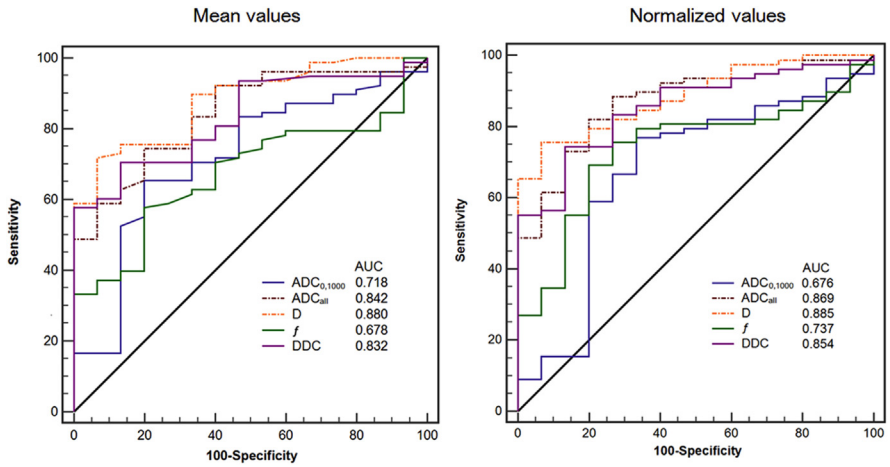

Figure 5 ROC curves for the mean and normalised diffusion metrics in distinguishing high-grade from low-grade meningiomas.

Table 5
p-Values from comparisons of areas under the curves among diffusion metrics for differentiating low-grade from high-grade meningiomas.

Mean values	$ADC_{0,1000}$	ADC_{all}	D	*f*	Normalised values	$ADC_{0,1000}$	ADC_{all}	D	*f*
ADC_{all}	0.012[a]	…	…	…	ADC_{all}	0.004[a]	…	…	…
D	0.004[a]	0.071	…	…	D	0.018[a]	0.609	…	…
f	0.493	0.004[a]	0.004[a]	…	*F*	0.337	0.003[a]	0.015[a]	…
DDC	0.047[a]	0.627	0.030[a]	0.009[a]	DDC	0.016[a]	0.358	0.282	0.015[a]

[a] $p<0.05$.
See Table 2 for definitions of abbreviations.

measurements.[18] D presents the perfusion-free diffusion and reflects the true diffusion coefficient. Therefore, D may be more helpful than ADC in grading meningioma. After analysing the D-values by ROC curve, a mean D-value of 0.522 mm^2/s and a normalised D-value of 1.181 were able to grade meningiomas with high AUC areas (0.880 and 0.885). These results were consistent with a previous study, suggesting that D is a reliable diagnostic marker.[10] In the present study, the D* value of high-grade meningiomas was slightly higher than that of low-grade meningiomas, but the difference was not significant. According to previous studies, D* is a perfusion-related parameter reflecting the capillary blood velocity.[18] The present findings suggest that D* is not the main influencing factor of ADC as ADC of high-grade meningiomas was still significantly lower than that of low-grade meningiomas as discussed above. Besides, several studies had reported D* might not be a reliable parameter because of its weak repeatability.[34,35] In the current study, the *f*-values of high-grade meningiomas were significantly lower than those of low-grade meningiomas. As the *f*-values correlate with the fractional volume of capillary blood flowing and blood vessel density, the lower *f*-values suggest decreased micro-perfusion within high-grade meningiomas.[36] Similarly, Lu *et al.* also reported that atypical meningiomas exhibited lower *f*-values than benign meningiomas[10]; however, one previous study reported that the estimate of *f* derived from BEM diffusion showed a poor measurement reproducibility.[37] Thus, conventional perfusion measurement techniques, such as DSC-MRI and ASL, may be more suitable for grading meningiomas.

According to the present results, DDC derived from SEM showed similar results to ADC and D, with lower estimates for high-grade meningiomas compared with low-grade meningiomas. SEM is another non-MEM that can provide information on diffusion and heterogeneity in tumours.[23] Although it was shown to be successful in tissue characterisation of various neoplasm, there is no study using SEM in grading meningiomas. DDC is considered as the weighted sum over the continuous distribution of ADCs that represent the multi-exponential decay properties.[38] In the current study, the lower DDC values in high-grade meningiomas were in line with the pathological characteristics of aggressive tumours, which usually demonstrated increased mitotic activity, necrosis, nuclear atypia, and small cells with increased intracellular complex protein molecules and nucleus to cytoplasm ratio.[39] In addition, the alpha values obtained from SEM showed no significant difference between high-grade and low-grade meningiomas in the present study. Alpha is regarded as a reflection of the microstructural heterogeneity of the tumour. Former research indicated that alpha could be used in evaluating the grade of gliomas and differentiated degree of nasopharyngeal cancer[14,24]; however, consistent with the current study, Lin *et al.* did not find a difference between poorly differentiated and well/moderately differentiated uterine cervical carcinomas.[40] The heterogeneity of alpha among studies suggests that the value of alpha varied among different types of tumours, and further larger cohort studies are needed.

Parameters derived from MEM, BEM, and SEM can provide diversified information. To the authors' knowledge, this is the first study to compare diffusion parameters derived from three different exponential models in grading meningiomas. Although various parameters showed statistically significant differences between low-grade and high-grade meningiomas, D and DDC had significantly better diagnostic performances than *f* in the differentiation. Moreover, D was the most significant parameter in meningioma grading. This might be explained by the fact that D is the pure molecular diffusion coefficient, thus it can avoid the bias of microcirculation contributions and represent the cellularity of tumours more precisely.[17] Hence, D obtained from BEM may be a more appropriate diffusion metric for assessing the grade of meningiomas; however, BEM diffusion needs relatively long acquisition and analyse times. Recently, some researchers have suggested that the imaging sequence could be abbreviated to as few as three b-values.[41,42] Thus, an optimised diffusion protocol may benefit the clinical practice for grading meningiomas in the future.

This study still has several limitations. Firstly, the sample size of high-grade meningiomas was relatively small; a larger and multicentre study population may further verify the present findings. Secondly, the number of b-values in the low spectrum was relatively small, but the b-values (<200 s/mm^2) used in this study have been proven to be useful for the evaluation of gliomas, sinonasal malignancies, and cervical cancers.[14,20,43] Thirdly, the association of diffusion parameters with pathological characteristics was not performed in this study. Detailed histological parameters, such as the cell density and nuclear to cytoplasmic ratio, should be explored in the future. Fourthly, the ROIs were drawn on a single section instead of the entire tumours, which might not reflect the characterisation of the whole tumours. Therefore, 3D ROIs should be measured in future studies.

In conclusion, different models of DWI, including MEM, BEM, and SEM, are useful in the differentiation between high-grade and low-grade meningiomas. Moreover, D and DDC have significantly better diagnostic performances than *f*. In addition, D obtained from BEM is the most promising diffusion parameter for predicting the grade of meningiomas.

Conflict of interest

The authors declare no conflict of interest.

Acknowledgements

This work was supported by a grant from the Shanghai Rising-Star Program (grant no. 16QA1400900); Shanghai Municipal Commission of Health and Family Planning (grant no. 2017BR003); Fujian Provincial Health and Family Planning Research Talent Training Program (grant no. 2017-2-24); Startup Fund for Scientific Research, Fujian Medical University, China (grant no. 2017XQ1036).

References

1. Louis DN, Perry A, Reifenberger G, *et al*. The 2016 World Health organization classification of tumors of the central nervous system: a summary. *Acta Neuropathol* Jun 2016;**131**(6):803–20.
2. Perry A, Stafford SL, Scheithauer BW, *et al*. Meningioma grading: an analysis of histologic parameters. *Am J Surg Pathol* 1997;**21**(12):1455–65.
3. Champeaux C, Dunn L. World Health Organization Grade II meningioma: a 10-year retrospective study for recurrence and prognostic factor assessment. *World Neurosurg* 2016;**89**:180–6.
4. Zhu H, Xie Q, Zhou Y, *et al*. Analysis of prognostic factors and treatment of anaplastic meningioma in China. *J Clin Neurosci* 2015;**22**(4):690–5.
5. Nabors LB, Portnow J, Ammirati M, *et al*. Central nervous system cancers, version 1.2015. *J Natl Compr Canc Netw* 2015;**13**(10):1191–202.
6. Watanabe Y, Yamasaki F, Kajiwara Y, *et al*. Preoperative histological grading of meningiomas using apparent diffusion coefficient at 3 T MRI. *Eur J Radiol* 2013;**82**(4):658–63.
7. Kawahara Y, Nakada M, Hayashi Y, *et al*. Prediction of high-grade meningioma by preoperative MRI assessment. *J Neurooncol* 2012;**108**(1):147–52.
8. Lin BJ, Chou KN, Kao HW, *et al*. Correlation between magnetic resonance imaging grading and pathological grading in meningioma. *J Neurosurg* 2014;**121**(5):1201–8.
9. Lin L, Bhawana R, Xue Y, *et al*. Comparative analysis of diffusional kurtosis imaging, diffusion tensor imaging, and diffusion-weighted imaging in grading and assessing cellular proliferation of meningiomas. *AJNR Am J Neuroradiol* 2018;**39**(6):1032–8.
10. Yiping L, Kawai S, Jianbo W, *et al*. Evaluation parameters between intravoxel incoherent motion and diffusion-weighted imaging in grading and differentiating histological subtypes of meningioma: a prospective pilot study. *J Neurol Sci* 2017;**372**:60–9.
11. Gihr GA, Horvath-Rizea D, Garnov N, *et al*. Diffusion profiling via a histogram approach distinguishes low-grade from high-grade meningiomas, can reflect the respective proliferative potential and progesterone receptor status. *Mol Imaging Biol* 2018;**20**(4):632–40.
12. Surov A, Ginat DT, Sanverdi E, *et al*. Use of diffusion weighted imaging in differentiating between malignant and benign meningiomas. A multicenter analysis. *World Neurosurg* 2016;**88**:598–602.
13. Le Bihan D, Breton E, Lallemand D, *et al*. Separation of diffusion and perfusion in intravoxel incoherent motion MR imaging. *Radiology* 1988;**168**(2):497–505.
14. Bai Y, Lin Y, Tian J, *et al*. Grading of gliomas by using monoexponential, biexponential, and stretched exponential diffusion-weighted MR imaging and diffusion kurtosis MR imaging. *Radiology* 2016;**278**(2):496–504.
15. Rheinheimer S, Stieltjes B, Schneider F, *et al*. Investigation of renal lesions by diffusion-weighted magnetic resonance imaging applying intravoxel incoherent motion-derived parameters—initial experience. *Eur J Radiol* 2012;**81**(3):e310–6.
16. Liu X, Zhou L, Peng W, *et al*. Comparison of stretched-exponential and monoexponential model diffusion-weighted imaging in prostate cancer and normal tissues. *J Magn Reson Imaging* 2015;**42**(4):1078–85.
17. Le Bihan D, Breton E, Lallemand D, *et al*. MR imaging of intravoxel incoherent motions: application to diffusion and perfusion in neurologic disorders. *Radiology* 1986;**161**(2):401–7.
18. Le Bihan D. Intravoxel incoherent motion perfusion MR imaging: a wake-up call. *Radiology* 2008;**249**(3):748–52.
19. Federau C, Meuli R, O'Brien K, *et al*. Perfusion measurement in brain gliomas with intravoxel incoherent motion MRI. *AJNR Am J Neuroradiol* 2014;**35**(2):256–62.
20. Xiao Z, Tang Z, Qiang J, *et al*. Intravoxel incoherent motion MR imaging in the differentiation of benign and malignant sinonasal lesions: comparison with conventional diffusion-weighted MR imaging. *AJNR Am J Neuroradiol* 2018;**39**(3):538–46.
21. Li H, Liang L, Li A, *et al*. Monoexponential, biexponential, and stretched exponential diffusion-weighted imaging models: quantitative biomarkers for differentiating renal clear cell carcinoma and minimal fat angiomyolipoma. *J Magn Reson Imaging* 2017;**46**(1):240–7.
22. Liu C, Liang C, Liu Z, *et al*. Intravoxel incoherent motion (IVIM) in evaluation of breast lesions: comparison with conventional DWI. *Eur J Radiol* 2013;**82**(12):e782–9.

23. Bennett KM, Schmainda KM, Bennett RT, *et al*. Characterization of continuously distributed cortical water diffusion rates with a stretched-exponential model. *Magn Reson Med* 2003;**50**(4):727–34.
24. Lai V, Lee VH, Lam KO, *et al*. Intravoxel water diffusion heterogeneity MR imaging of nasopharyngeal carcinoma using stretched exponential diffusion model. *Eur Radiol* 2015;**25**(6):1708–13.
25. Winfield JM, deSouza NM, Priest AN, *et al*. Modelling DW-MRI data from primary and metastatic ovarian tumours. *Eur Radiol* 2015;**25**(7):2033–40.
26. Bihan DL. Molecular diffusion, tissue microdynamics and microstructure. *Nmr Biomed* 1995;**8**(7):375–86.
27. Jiang R, Jiang J, Zhao L, *et al*. Diffusion kurtosis imaging can efficiently assess the glioma grade and cellular proliferation. *Oncotarget* 2015;**6**(39):42380–93.
28. Baskan O, Silav G, Bolukbasi FH, *et al*. Relation of apparent diffusion coefficient with Ki-67 proliferation index in meningiomas. *Br J Radiol* 2016;**89**(1057):20140842.
29. Dyvorne HA, Galea N, Nevers T, *et al*. Diffusion-weighted imaging of the liver with multiple b values: effect of diffusion gradient polarity and breathing acquisition on image quality and intravoxel incoherent motion parameters—a pilot study. *Radiology* 2013;**266**(3):920–9.
30. Le BD. Apparent diffusion coefficient and beyond: what diffusion MR imaging can tell us about tissue structure. *Radiology* 2013;**268**(2):318–22.
31. Filippi CG, Edgar MA, Ulug AM, *et al*. Appearance of meningiomas on diffusion-weighted images: correlating diffusion constants with histopathologic findings. *AJNR Am J Neuroradiol* 2001;**22**(1):65–72.
32. Sanverdi SE, Ozgen B, Oguz KK, *et al*. Is diffusion-weighted imaging useful in grading and differentiating histopathological subtypes of meningiomas? *Eur J Radiol* 2012;**81**(9):2389–95.
33. Thoeny HC, De Keyzer F, Boesch C, *et al*. Diffusion-weighted imaging of the parotid gland: influence of the choice of b-values on the apparent diffusion coefficient value. *J Magn Reson Imaging* 2004;**20**(5):786–90.
34. Chiaradia M, Baranes L, Van Nhieu JT, *et al*. Intravoxel incoherent motion (IVIM) MR imaging of colorectal liver metastases: are we only looking at tumor necrosis? *J Magn Reson Imaging* 2014;**39**(2):317–25.
35. Togao O, Hiwatashi A, Yamashita K, *et al*. Measurement of the perfusion fraction in brain tumors with intravoxel incoherent motion MR imaging: validation with histopathological vascular density in meningiomas. *Br J Radiol* 2018;**91**(1085):20170912.
36. Shinmoto H, Tamura C, Soga S, *et al*. An intravoxel incoherent motion diffusion-weighted imaging study of prostate cancer. *AJR Am J Roentgenol* 2012;**199**(4):W496–500.
37. Andreou A, Koh DM, Collins DJ, *et al*. Measurement reproducibility of perfusion fraction and pseudodiffusion coefficient derived by intravoxel incoherent motion diffusion-weighted MR imaging in normal liver and metastases. *Eur Radiol* 2013;**23**(2):428–34.
38. Bennett KM, Hyde JS, Schmainda KM. Water diffusion heterogeneity index in the human brain is insensitive to the orientation of applied magnetic field gradients. *Magn Reson Med* 2006;**56**(2):235.
39. Nagar VA, Ye JR, Ng WH, *et al*. Diffusion-weighted MR imaging: diagnosing atypical or malignant meningiomas and detecting tumor dedifferentiation. *Ajnr Am J Neuroradiol* 2008;**29**(6):1147–52.
40. Lin M, Yu X, Chen Y, *et al*. Contribution of mono-exponential, bi-exponential and stretched exponential model-based diffusion-weighted MR imaging in the diagnosis and differentiation of uterine cervical carcinoma. *Eur Radiol* 2017;**27**(6):2400–10.
41. Cao M, Suo S, Han X, *et al*. Application of a simplified method for estimating perfusion derived from diffusion-weighted MR imaging in glioma grading. *Front Aging Neurosci* 2017;**9**:432.
42. Murtz P, Sprinkart AM, Reick M, *et al*. Accurate IVIM model-based liver lesion characterisation can be achieved with only three b-value DWI. *Eur Radiol* 2018;**28**(10):4418–28.
43. Wu Q, Zheng D, Shi L, *et al*. Differentiating metastatic from non-metastatic lymph nodes in cervical cancer patients using mono-exponential, biexponential, and stretched exponential diffusion-weighted MR imaging. *Eur Radiol* 2017;**27**(12):5272–9.